

# Hydro-morphodynamics 2D modelling using a discontinuous Galerkin discretisation

---

**Mariana Clare\***

Co-authors: Dr James Percival\*, Dr Stephan Kramer\*, Dr Athanasios Angeloudis\*\*, Prof. Colin Cotter\* & Prof. Matthew Piggott\*

\*Imperial College London \*\*University of Edinburgh

**EGU2020: Sharing Geoscience Online, 6<sup>th</sup> May 2020**

**EPSRC**  
Engineering and Physical Sciences  
Research Council



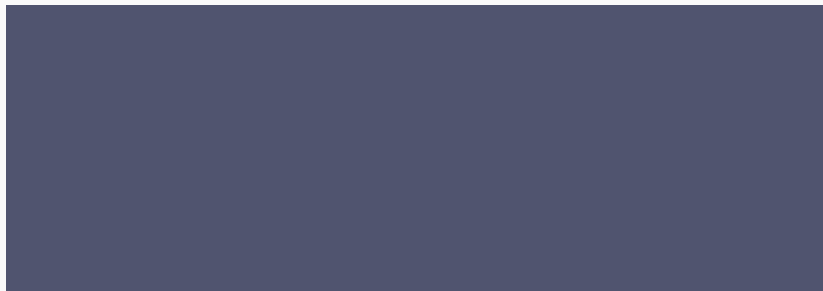
**Imperial College  
London**

The first three sections of this presentation present work published in  
*Clare, M., Percival, J., Angeloudis, A., Cotter, C., & Piggott, M. (2020, January 9). Hydro-morphodynamics 2D modelling using a discontinuous Galerkin discretisation. <https://doi.org/10.31223/osf.io/tpqvy>*

Any questions or comments on this presentation are very welcome.  
The authors can be contacted either during the live chat on 6<sup>th</sup> May 2020 or by emailing *[m.clare17@imperial.ac.uk](mailto:m.clare17@imperial.ac.uk)*

# MOTIVATION

Data from 2010 shows almost 400 million people lived in areas less than 5m above average sea level. As sea levels rise and storms increase in strength and frequency due to climate change, the coastal zone is becoming a critical location for advanced mathematical techniques.



February 2014 storm in Dawlish, Devon. The damage cost £35 million to repair and the closure of the train link cost the Cornish economy an estimated £1.2 billion.

*N.B.: It may be necessary to enable 3D content in Adobe Acrobat to play this video.*

# SECTION OVERVIEW

## Section 1:

Building a hydro-morphodynamics 2D model in *Thetis*

## Section 2:

Migrating Trench

## Section 3

Meander

## Section 4

Adjoint Method

## Summary

## **Section 1:**

Building a  
hydro-morphodynamics 2D  
model in *Thetis*

---

## 1.1 BASIC MODEL EQUATIONS

The hydrodynamic component of the model is governed by the shallow water equations and they are coupled with the equation for conservation of suspended sediment

$$\frac{\partial}{\partial t}(hC) + \frac{\partial}{\partial x}(hF_{corr}U_1C) + \frac{\partial}{\partial y}(hF_{corr}U_2C) = \frac{\partial}{\partial x} \left[ h \left( \epsilon_s \frac{\partial C}{\partial x} \right) \right] + \frac{\partial}{\partial y} \left[ h \left( \epsilon_s \frac{\partial C}{\partial y} \right) \right] + E_b - D_b. \quad (1)$$

The new bedlevel ( $z_b$ ) is governed by the Exner equation

$$\frac{(1 - p')}{m} \frac{dz_b}{dt} + \nabla_h \cdot \mathbf{Q}_b = D_b - E_b. \quad (2)$$

Here  $\epsilon_s$  is the diffusivity constant,  $E_b - D_b$  the source term,  $F_{corr}$  a correction factor (see *Clare et al. (2020)*),  $\mathbf{Q}_b$  the bedload transport and  $m$  a morphological acceleration factor.

## 1.2 ADDING PHYSICAL EFFECTS

The formulation of  $Q_b$  ignores various physical effects which are added here:

### Slope Effect

$Q_b$  will be less than predicted for a positive gradient bed because gravity acts against the flow (and vice-versa). Thus, a magnitude correction is needed

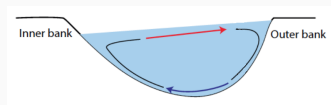
$$Q_{b*} = Q_b \left( 1 - \tau \frac{\partial z_b}{\partial s} \right),$$

as well as a correction on the flow direction (where  $\delta$  is the original angle)

$$\tan \alpha = \tan \delta - T \frac{\partial z_b}{\partial n}.$$

### Secondary Current

The helical flow effect in curved channels is accounted for by the addition of a secondary current

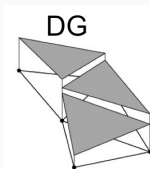


## 1.3 THETIS

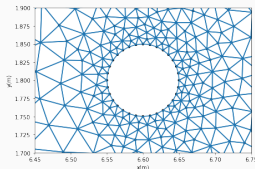
Our model is built using *Thetis*, a finite element coastal ocean model built using the code generating framework *Firedrake* (see *Kärnä et al. (2016)*).

We use a **discontinuous Galerkin (DG)** finite element discretisation which is

- + Locally mass conservative;
- + Well-suited to advection dominated problems;
- + Geometrically flexible;
- + Allows higher order local approximations.



DG setup



Example mesh

This is the first use of DG with a full hydro-morphodynamics model.



## **Section 2:**

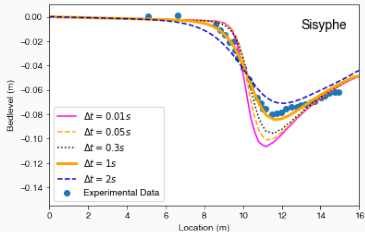
### Migrating Trench

---

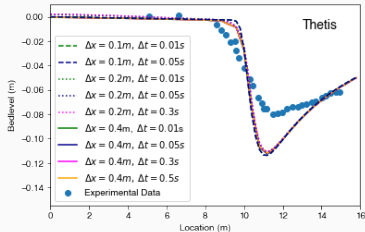
## 2.1 MIGRATING TRENCH

We verify and validate our model with the migrating trench test case using both the industry standard model *Sisyphé* and experimental data (see *Villaret et al. (2016)*).

*Sisyphé*'s results vary significantly with  $\Delta t$ , converging only as  $\Delta t$  decreases. On the other hand, *Thetis*' results are unaltered by changes to  $\Delta t$  and are thus much more robust, a fundamental advantage of our model.



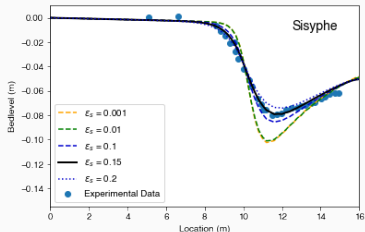
*Sisyphé* greatly affected by changes to  $\Delta t$



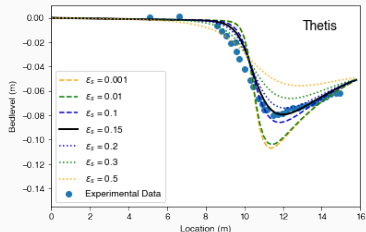
*Thetis* insensitive to changes in  $\Delta t$

## 2.2 MIGRATING TRENCH: VARYING DIFFUSIVITY

Using the current parameters, neither model matches with the experimental data. However, both models are sensitive to changes in the diffusivity constant  $\epsilon_s$  in (1), and match the experimental data when this parameter is correctly calibrated.



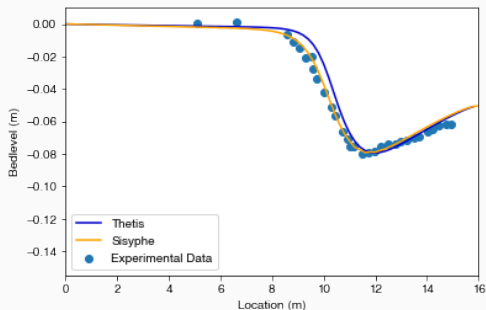
*Sensitivity of Sisyphus to  $\epsilon_s$*



*Sensitivity of Thetis to  $\epsilon_s$*

## 2.3 MIGRATING TRENCH: FINAL RESULT

Thus, our *Thetis* results match both the experimental data and *Sisyphé's*, using a calibrated  $\epsilon_S$  in both models and a small enough  $\Delta t$  in *Sisyphé*.



*Bedlevel from Thetis and Sisyphé after 15 h*

## 2.4 MIGRATING TRENCH: SIMULATION



*N.B.: It may be necessary to enable 3D content in Adobe Acrobat to play this video.*

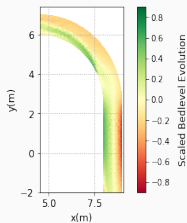
## **Section 3**

### Meander

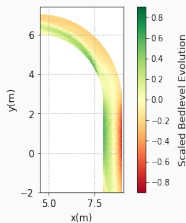
---

## 3.1 MEANDER

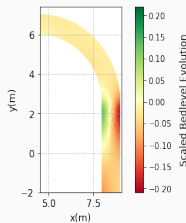
A meander is a much more complex test case and allows us to verify and validate the physical effects corrections, especially the implementation of the secondary current. Using the same set-up as in *Villaret et al. (2013)*, we show how these effects change the final bedlevel:



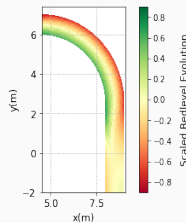
*No physical corrections*



*Only slope effect magnitude*



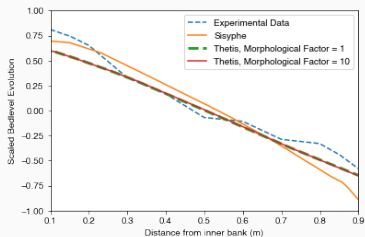
*Both slope effect corrections*



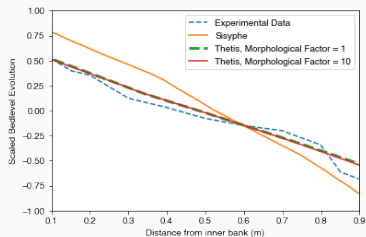
*All physical corrections*

## 3.2 MEANDER: RESULTS

We again find that *Sisyphé* is sensitive to changes in  $\Delta t$ , whereas *Thetis* is robust (see *Clare et al. (2020)*). Furthermore, we find that *Thetis* approximates the experimental data more accurately.



Cross-section at 90°



Cross-section at 180°

Comparing scaled bedlevel evolution from *Thetis*, *Sisyphé* and experimental data



## 3.3 MEANDER: SIMULATION



*N.B.: It may be necessary to enable 3D content in Adobe Acrobat to play this video.*

## **Section 4**

### Adjoint Method

---

## 4.1 ADJOINT METHOD

Hydro-morphodynamics models have a large degree of uncertainty associated with them, partly due to incomplete knowledge of physical parameters.

The adjoint method is used to compute gradients of model outputs,  $\mathbf{u}$ , with respect to these uncertain input parameters,  $m$ . It has the following key advantages:

- increasing the number of uncertain parameters has **no effect** on the computational cost;
- no assumptions are made about the distribution of the input parameters or outputs.

Our model has the further advantage that *Thetis* has a fully flexible free-to-use adjoint component available, thus making the adjoint method simple to use.

## 4.2 MINIMIZING OUTPUT FUNCTIONAL

We thus use the adjoint method for calibration by minimizing the output functional

$$J(\mathbf{u}^{\text{model}}, \mathbf{m}) := \frac{1}{2} \sum_{j=1}^{N_{\text{out}}} \int_0^T \int_{\Omega} |u_j^{\text{true}} - u_j^{\text{model}}|^2 dx dt + \sum_{i=1}^{N_{\text{in}}} \frac{\beta_i}{2} \int_0^T \int_{\Omega_m} |m_i|^2 dx dt,$$

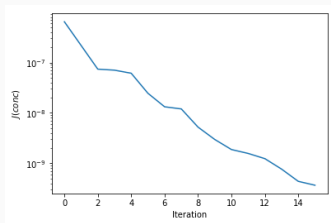
where the first integral is the difference between the true value and the model output, and the second integral is a Tikhonov regularisation term. The true value may be from

- real-world data;
- from a previous run of the model with a known value to verify that the parameter can be reconstructed (twin experiment).

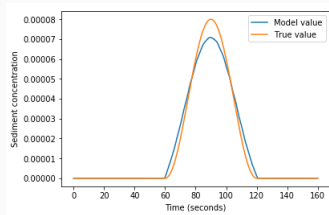
## 4.3 TWIN EXPERIMENT

To demonstrate adjoint capability, we introduce a sediment wave at the input boundary in the migrating trench set-up. We record the bedlevel after every couple of timesteps.

We then run the model again with no incoming sediment and use the adjoint method to minimize the output functional up to a given tolerance. We are able to reconstruct the true value very closely.



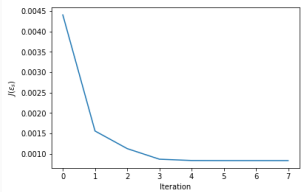
Minimization of output functional with  
 $\beta_i = 2$



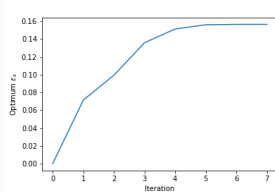
Comparison of optimised model value  
with true value of input sediment rate

## 4.4 CALIBRATION WITH DATA - A PRELIMINARY EXAMPLE

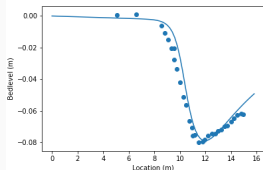
As we have already seen, the migrating trench is sensitive to the diffusivity constant,  $\epsilon_s$ . We use the adjoint method to calibrate this parameter successfully, using the bedlevel experimental data as the real data (note there is no need for a regularisation term here as this is a single parameter).



Minimization of output functional



Convergence to optimised  $\epsilon_s$



Bedlevel with optimum  $\epsilon_s$

# Summary





---

# SUMMARY

1. We present the first full hydro-morphodynamics model employing a DG based discretisation;
2. Validate our model for two different test cases;
3. Show our model is both accurate and stable, and has key advantages in robustness and accuracy over the industry standard *Sisyphe*;
4. Show how the adjoint method can be used to calibrate our model and reduce input parameter uncertainty.



# KEY REFERENCES

-  Funke, S., Farrell, P., Piggott, M., 2017. 'Reconstructing wave profiles from inundation data', *Computer Methods in Applied Mechanics and Engineering*, **322**, 167–186.
-  Kärnä, T., Kramer, S.C., Mitchell, L., Ham, D.A., Piggott, M.D. and Baptista, A.M. (2018), 'Thetis coastal ocean model: discontinuous Galerkin discretization for the threedimensional hydrostatic equations', *Geoscientific Model Development*, **11**, 4359-4382.
-  Villaret, C., Hervouet, J.-M., Kopmann, R., Merkel, U., and Davies, A. G. (2013), 'Morphodynamic modeling using the telemac finite-element system', *Computers & Geosciences*, **53**, 105-113.
-  Villaret, C., Kopmann, R., Wyncoll, D., Riehme, J., Merkel, U. and Naumann, U. (2016), 'First-order uncertainty analysis using Algorithmic Differentiation of morphodynamic models', *Computers & Geosciences*, **90**, 144-151.